

Nuclear lattice simulations

Dean Lee^{*,a,b}, Evgeny Epelbaum^{c,b}, Hermann Krebs^{b,c}, Ulf-G. Meißner^{b,c,d}

^aDepartment of Physics, North Carolina State University, Raleigh, NC 27695, USA

*^bHelmholtz-Institut für Strahlen- und Kernphysik (Theorie) and
Bethe Center for Theoretical Physics, Universität Bonn, D-53115 Bonn, Germany*

*^cInstitut für Kernphysik (IKP-3) and Jülich Center for Hadron Physics,
Forschungszentrum Jülich, D-52425 Jülich, Germany*

*^dInstitute for Advanced Simulations (IAS),
Forschungszentrum Jülich, D-52425 Jülich, Germany*

*E-mail: dean_lee@ncsu.edu, e.epelbaum@fz-juelich.de,
h.krebs@fz-juelich.de, meissner@itkp.uni-bonn.de*

We summarize recent progress on nuclear lattice simulations using chiral effective field theory. We present lattice results for dilute neutron matter at next-to-leading order and three-body forces in light nuclei at next-to-next-to-leading order.

*6th International Workshop on Chiral Dynamics
July 6-10 2009
Bern, Switzerland*

*Speaker.

1. Introduction

Lattice simulations based on low-energy effective field theory have been used in studies of nuclear matter [1] and neutron matter [2, 3, 4, 5, 6, 7]. The method has also been applied to light nuclei in pionless effective field theory [8] and chiral effective field theory at leading order (LO) [9]. More recently next-to-leading order (NLO) calculations have been carried out for the ground state of neutron matter [10, 11]. A review of lattice effective field theory calculations can be found in Ref. [12].

At leading order in chiral effective field theory the nucleon-nucleon effective potential is

$$V_{\text{LO}} = V + V_{I^2} + V^{\text{OPEP}}. \quad (1.1)$$

V , V_{I^2} are the two independent contact interactions at leading order in the Weinberg power counting scheme, and V^{OPEP} is the instantaneous one-pion exchange potential. The interactions in V_{LO} can be described in terms of their matrix elements with two-nucleon incoming and outgoing momentum states. For bookkeeping purposes we label the amplitude as though the two interacting nucleons were distinguishable, A and B . In the following we use $\vec{\sigma}$ to signify the Pauli matrices for spin and $\vec{\tau}$ to indicate the Pauli matrices for isospin.

For the two leading-order contact interactions the amplitudes are

$$\mathcal{A}(V) = C, \quad (1.2)$$

$$\mathcal{A}(V_{I^2}) = C_{I^2} \vec{\tau}_A \cdot \vec{\tau}_B. \quad (1.3)$$

For the one-pion exchange potential,

$$\mathcal{A}(V^{\text{OPEP}}) = - \left(\frac{g_A}{2f_\pi} \right)^2 \frac{(\vec{\tau}_A \cdot \vec{\tau}_B) (\vec{q} \cdot \vec{\sigma}_A) (\vec{q} \cdot \vec{\sigma}_B)}{q^2 + m_\pi^2}. \quad (1.4)$$

Here m is the nucleon mass, m_π the pion mass, f_π the pion decay constant, and g_A the nucleon axial charge.

In Ref. [9] two different lattice actions were considered which were later denoted LO_1 and LO_2 [10]. The interactions in V_{LO_1} include one-pion exchange and two zero-range contact interactions corresponding with amplitude

$$\mathcal{A}(V_{\text{LO}_1}) = C + C_{I^2} \vec{\tau}_A \cdot \vec{\tau}_B + \mathcal{A}(V^{\text{OPEP}}). \quad (1.5)$$

The interactions in V_{LO_2} consist of one-pion exchange and two Gaussian-smearred contact interactions,

$$\mathcal{A}(V_{\text{LO}_2}) = C f(\vec{q}) + C_{I^2} f(\vec{q}) \vec{\tau}_A \cdot \vec{\tau}_B + \mathcal{A}(V^{\text{OPEP}}), \quad (1.6)$$

where $f(\vec{q})$ is a lattice approximation to a Gaussian function. The smeared interactions in LO_2 were used to better reproduce S -wave phase shifts for nucleon momenta up to the pion mass.

In Ref. [10] phase shifts were calculated for these two lattice actions using the spherical wall method [13] at spatial lattice spacing $a = (100 \text{ MeV})^{-1}$ and temporal lattice spacing $a_t = (70 \text{ MeV})^{-1}$. NLO corrections were also computed and the unknown operator coefficients determined by fitting to low-energy nucleon-nucleon scattering data.

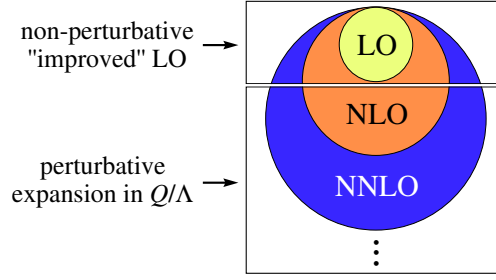


Figure 1: The “improved” LO action is iterated non-perturbatively while the remaining higher-order interactions are treated using perturbation theory.

The replacement of pointlike interactions in LO_1 with Gaussian-smearred interactions in LO_2 is similar to the lattice improvement program of Symanzik used in lattice QCD actions [14, 15]. There is a conceptual difference however since we are dealing with an effective field theory rather than a renormalizable field theory. The higher-order operators we consider do not only cancel lattice artifacts but also include higher-order interactions of the effective theory. In our lattice calculations the improved leading-order action is treated non-perturbatively while higher-order interactions are included as a perturbative expansion. The choice of improved action sets a dividing line between perturbative and non-perturbative interactions. This is sketched in Fig. 1. The dividing line should be immaterial so long as the perturbative expansion converges. At any given order, lattice calculations using different improved actions should agree up to corrections the size of terms at next order.

2. Dilute neutrons at next-to-leading order

In Ref. [11] the ground state energy for dilute neutron matter was computed using the lattice action LO_2 and auxiliary-field Monte Carlo. Next-to-leading-order corrections to the energy were also calculated. In this calculation the dominant source of systematic error was the large size of NLO corrections for Fermi momenta larger than 100 MeV. The problem is caused by attractive P -wave interactions introduced by Gaussian smearing in LO_2 that must be cancelled by NLO corrections. In systems with both protons and neutrons this P -wave correction is numerically small when compared with the strong binding produced by S -wave interactions. For pure neutron matter, however, the P -wave interactions are not as small an effect in relative terms.

These problems were resolved using a new leading-order action LO_3 introduced in Ref. [16]. The interactions in V_{LO_3} correspond with the amplitude,

$$\begin{aligned} \mathcal{A}(V_{LO_3}) = & C_{S=0,I=1} f(\vec{q}) \left(\frac{1}{4} - \frac{1}{4} \vec{\sigma}_A \cdot \vec{\sigma}_B \right) \left(\frac{3}{4} + \frac{1}{4} \vec{\tau}_A \cdot \vec{\tau}_B \right) \\ & + C_{S=1,I=0} f(\vec{q}) \left(\frac{3}{4} + \frac{1}{4} \vec{\sigma}_A \cdot \vec{\sigma}_B \right) \left(\frac{1}{4} - \frac{1}{4} \vec{\tau}_A \cdot \vec{\tau}_B \right) + \mathcal{A}(V^{OPEP}). \end{aligned} \quad (2.1)$$

The Gaussian-smearred interactions are multiplied by spin and isospin projection operators. Only the $C_{S=0,I=1}$ term contributes in pure neutron matter. Using the LO_3 action with NLO corrections,

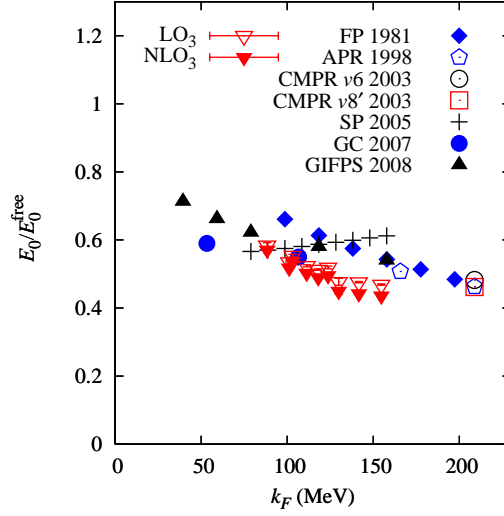


Figure 2: Ground state energy ratio E_0/E_0^{free} for LO₃ and NLO₃ versus Fermi momentum k_F . For comparison we show results for FP 1981 [17], APR 1998 [18], CMPR v6 and v8' 2003 [19], SP 2005 [20], GC 2007 [21], and GIFPS 2008 [22].

we have computed the ground state energy for dilute neutrons in a periodic box [16]. For spatial lattice spacing $a = (100 \text{ MeV})^{-1}$ and temporal lattice spacing $a_t = (70 \text{ MeV})^{-1}$ simulations were done with 8, 12, 16 neutrons in periodic boxes with lengths $L = 4, 5, 6, 7$. In Fig. 2 we show results for the ratio of the interacting ground state energy to non-interacting ground state energy, $E_{0,\text{NLO}}/E_0^{\text{free}}$, as a function of Fermi momentum k_F . For comparison we show other results from the literature: FP 1981 [17], APR 1998 [18], CMPR v6 and v8' [19], SP 2005 [20], GC 2007 [21], and GIFPS 2008 [22].

3. Three-body forces in light nuclei at next-to-next-to-leading order

A number of different phenomenological three-nucleon potentials have been investigated in the literature [23, 24, 25, 26, 27, 28, 29, 30, 31]. Effective field theory provides a systematic method for estimating the relative importance of three-body interaction terms. Few-nucleon forces in chiral effective field theory beyond two nucleons were first introduced in Ref. [32]. In Ref. [33] it was shown that three-nucleon interactions at NLO cancel and three-body effects first appear at NNLO. The NNLO three-nucleon effective potential includes a pure contact potential, $V_{\text{contact}}^{(3N)}$, one-pion exchange potential, $V_{\text{OPE}}^{(3N)}$, and a two-pion exchange potential, $V_{\text{TPE}}^{(3N)}$,

$$V_{\text{NNLO}}^{(3N)} = V_{\text{contact}}^{(3N)} + V_{\text{OPE}}^{(3N)} + V_{\text{TPE}}^{(3N)}. \quad (3.1)$$

The corresponding diagrams are shown in Fig. 3.

Similar to our bookkeeping notation for two-nucleon interactions, we write the tree-level amplitude for three-nucleon interactions where the first nucleon is type A , the second nucleon type B , and the third type C . We sum over all permutations $P(A, B, C)$ of the labels, and $\vec{q}_A, \vec{q}_B, \vec{q}_C$

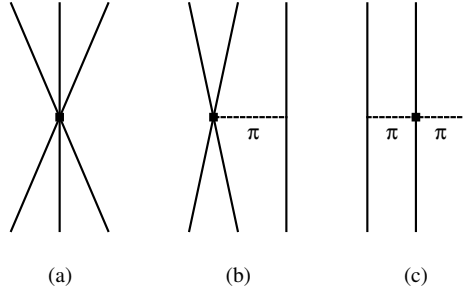


Figure 3: Three-nucleon forces at NNLO. Diagrams (a), (b), and (c) show the contact potential, $V_{\text{contact}}^{(3N)}$, one-pion exchange potential $V_{\text{OPE}}^{(3N)}$, and two-pion exchange potential $V_{\text{TPE}}^{(3N)}$.

are defined as the differences between final and initial momenta for the respective nucleons. The amplitudes for $V_{\text{contact}}^{(3N)}$ and $V_{\text{OPE}}^{(3N)}$ are [34, 35]

$$\mathcal{A} \left[V_{\text{contact}}^{(3N)} \right] = \frac{1}{2} E \sum_{P(A,B,C)} (\vec{\tau}_A \cdot \vec{\tau}_B), \quad (3.2)$$

$$\mathcal{A} \left[V_{\text{OPE}}^{(3N)} \right] = -\frac{g_A}{8f_\pi^2} D \sum_{P(A,B,C)} \frac{\vec{q}_A \cdot \vec{\sigma}_A}{q_A^2 + m_\pi^2} (\vec{q}_A \cdot \vec{\sigma}_B) (\vec{\tau}_A \cdot \vec{\tau}_B). \quad (3.3)$$

The coefficients E and D are both cutoff dependent. The coefficient E determines the short distance interactions between three nucleons, while D determines the pion coupling to two nucleons. Following the notation introduced in Ref. [35], we define dimensionless parameters c_E and c_D such that

$$E = \frac{c_E}{f_\pi^4 \Lambda_\chi}, \quad D = \frac{c_D}{f_\pi^2 \Lambda_\chi}, \quad (3.4)$$

where $\Lambda_\chi \simeq m_\rho$. We take $\Lambda_\chi = 700$ MeV.

For convenience we separately label three parts of the two-pion exchange potential,

$$V_{\text{TPE}}^{(3N)} = V_{\text{TPE1}}^{(3N)} + V_{\text{TPE2}}^{(3N)} + V_{\text{TPE3}}^{(3N)}. \quad (3.5)$$

The corresponding amplitudes are

$$\mathcal{A} \left[V_{\text{TPE1}}^{(3N)} \right] = \frac{c_3}{f_\pi^2} \left(\frac{g_A}{2f_\pi} \right)^2 \sum_{P(A,B,C)} \frac{(\vec{q}_A \cdot \vec{\sigma}_A) (\vec{q}_B \cdot \vec{\sigma}_B)}{(q_A^2 + m_\pi^2) (q_B^2 + m_\pi^2)} (\vec{q}_A \cdot \vec{q}_B) (\vec{\tau}_A \cdot \vec{\tau}_B), \quad (3.6)$$

$$\mathcal{A} \left[V_{\text{TPE2}}^{(3N)} \right] = -\frac{2c_1 m_\pi^2}{f_\pi^2} \left(\frac{g_A}{2f_\pi} \right)^2 \sum_{P(A,B,C)} \frac{(\vec{q}_A \cdot \vec{\sigma}_A) (\vec{q}_B \cdot \vec{\sigma}_B)}{(q_A^2 + m_\pi^2) (q_B^2 + m_\pi^2)} (\vec{\tau}_A \cdot \vec{\tau}_B), \quad (3.7)$$

$$\begin{aligned} \mathcal{A} \left[V_{\text{TPE3}}^{(3N)} \right] &= \frac{c_4}{2f_\pi^2} \left(\frac{g_A}{2f_\pi} \right)^2 \\ &\times \sum_{P(A,B,C)} \frac{(\vec{q}_A \cdot \vec{\sigma}_A) (\vec{q}_B \cdot \vec{\sigma}_B)}{(q_A^2 + m_\pi^2) (q_B^2 + m_\pi^2)} [(\vec{q}_A \times \vec{q}_B) \cdot \vec{\sigma}_C] [(\vec{\tau}_A \times \vec{\tau}_B) \cdot \vec{\tau}_C]. \end{aligned} \quad (3.8)$$

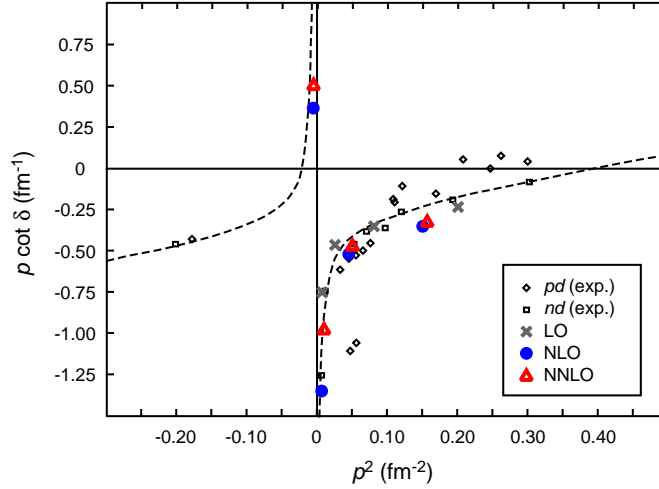


Figure 4: Plot of $p \cot \delta$ versus p^2 for spin-doublet nucleon-deuteron scattering in the center-of-mass frame. For the NNLO calculation we take $c_D = 1.0$ fitted to the physical value for E_{triton} . The experimental results are from Ref. [42].

The low-energy constants c_1, c_3, c_4 parameterize the coupling of the nucleon to two pions. These constants have been determined from fits to low-energy pion-nucleon scattering data [36], and in the following we use the values $c_1 = -0.81 \text{ GeV}^{-1}$, $c_3 = -4.7 \text{ GeV}^{-1}$, $c_4 = 3.4 \text{ GeV}^{-1}$ [37].

At fixed lattice spacing we constraint the two unknown coefficients by fitting to the triton binding energy and spin-doublet nucleon-deuteron scattering via Lüscher’s finite volume formula [38, 39, 40]. We fix the coefficient c_E as a function of c_D by matching the physical triton energy at infinite volume, -8.48 MeV . The value of c_D is then determined from the spin-doublet nucleon-deuteron scattering phase shifts. Results for the doublet nucleon-deuteron scattering phase shift are shown in Fig. 4 using the LO_2 lattice action for lattice spacing $a = (100 \text{ MeV})^{-1}$ and temporal lattice spacing $a_t = (150 \text{ MeV})^{-1}$ with $c_D = 1.0$ [41]. It turns out however that nucleon-deuteron scattering provides only a mild constraint on c_D . Currently other methods are being investigated for constraining c_D , including one recent suggestion to determine c_D from the triton beta decay rate [43].

Aside from the uncertainty in c_D , we have determined all interactions on the lattice up to NNLO including three-body forces. Using these interactions we have computed the ground state energy of the alpha particle without Coulomb interactions on a periodic lattice using auxiliary-field projection Monte Carlo [41]. In Fig. 5 we plot the NNLO α -particle energy versus c_D , with c_E fitted to the physical triton energy. The bands indicate the estimated error due to stochastic noise and asymptotic fits at large Euclidean projection time t . The α energy shown at -29.0 MeV is the estimated Coulomb-subtracted energy [31]. At large volumes the best agreement with the Coulomb-subtracted α energy occurs at $c_D \approx -4$. The α binding increases in strength by 0.2 MeV for each unit increase in c_D , and so we find reasonable agreement for all values of $c_D \sim O(1)$.

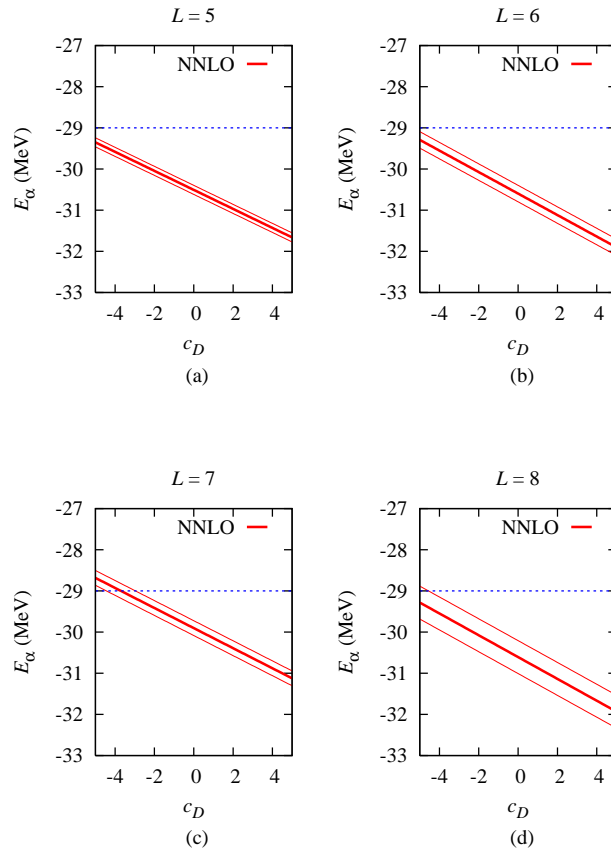


Figure 5: Energy of the α particle at NNLO versus c_D . The contact interaction c_E is fitted to the physical triton energy. The dotted line is the estimated Coulomb-subtracted energy -29.0 MeV.

Acknowledgements

Partial financial support from the Deutsche Forschungsgemeinschaft (SFB/TR 16), Helmholtz Association (contract number VH-NG-222 and VH-VI-231), and U.S. Department of Energy (DE-FG02-03ER41260) are acknowledged. This work was further supported by the EU Hadron-Physics2 project “Study of strongly interacting matter”. The computational resources for this project were provided by the Jülich Supercomputing Centre at the Forschungszentrum Jülich.

References

- [1] H. M. Müller, S. E. Koonin, R. Seki, and U. van Kolck, *Phys. Rev.* **C61** 044320, 2000.
- [2] D. Lee and T. Schäfer, *Phys. Rev.* **C72** 024006, 2005.
- [3] D. Lee, B. Borasoy, and T. Schäfer, *Phys. Rev.* **C70** 014007, 2004.
- [4] D. Lee and T. Schäfer, *Phys. Rev.* **C73** 015201, 2006.
- [5] D. Lee and T. Schäfer, *Phys. Rev.* **C73** 015202, 2006.
- [6] T. Abe and R. Seki, *Phys. Rev.* **C79** 054002, 2009.

- [7] T. Abe and R. Seki, *Phys. Rev.* **C79** 054003, 2009.
- [8] B. Borasoy, H. Krebs, D. Lee, and U.-G. Meißner, *Nucl. Phys.* **A768** 179–193, 2006.
- [9] B. Borasoy, E. Epelbaum, H. Krebs, D. Lee, and U.-G. Meißner, *Eur. Phys. J.* **A31** 105–123, 2007.
- [10] B. Borasoy, E. Epelbaum, H. Krebs, D. Lee, and U.-G. Meißner, *Eur. Phys. J.* **A35** 343–355, 2008.
- [11] B. Borasoy, E. Epelbaum, H. Krebs, D. Lee, and U.-G. Meißner, *Eur. Phys. J.* **A35** 357–367, 2008.
- [12] D. Lee, *Prog. Part. Nucl. Phys.* **63** 117–154, 2009.
- [13] B. Borasoy, E. Epelbaum, H. Krebs, D. Lee, and U.-G. Meißner, *Eur. Phys. J.* **A34** 185–196, 2007.
- [14] K. Symanzik, *Nucl. Phys.* **B226** 187, 1983.
- [15] K. Symanzik, *Nucl. Phys.* **B226** 205, 1983.
- [16] E. Epelbaum, H. Krebs, D. Lee, and U.-G. Meißner, *Eur. Phys. J.* **A40** 199–213, 2009.
- [17] B. Friedman and V. R. Pandharipande, *Nucl. Phys.* **A361** 502–520, 1981.
- [18] A. Akmal, V. R. Pandharipande, and D. G. Ravenhall, *Phys. Rev.* **C58** 1804–1828, 1998.
- [19] J. Carlson, J. Morales, V. R. Pandharipande, and D. G. Ravenhall, *Phys. Rev.* **C68** 025802, 2003.
- [20] A. Schwenk and C. J. Pethick, *Phys. Rev. Lett.* **95** 160401, 2005.
- [21] A. Gezerlis and J. Carlson, *Phys. Rev.* **C77** 032801, 2008.
- [22] S. Gandolfi, A. Y. Illarionov, S. Fantoni, F. Pederiva, and K. E. Schmidt, *Phys. Rev. Lett.* **101** 132501, 2008.
- [23] J. Fujita and H. Miyazawa, *Prog. Theor. Phys.* **17** 360–365, 1957.
- [24] B. H. J. McKellar and R. Rajaraman, *Phys. Rev. Lett.* **21(7)** 450–453, 1968.
- [25] S.-N. Yang, *Phys. Rev.* **C10** 2067–2079, 1974.
- [26] S. A. Coon, M. D. Scadron, and B. R. Barrett, *Nucl. Phys.* **A242** 467, 1975.
- [27] S. A. Coon et al, *Nucl. Phys.* **A317** 242–278, 1979.
- [28] S. A. Coon and W. Glöckle, *Phys. Rev.* **C23(4)** 1790–1802, 1981.
- [29] J. Carlson, V. R. Pandharipande, and R. B. Wiringa, *Nucl. Phys.* **A401** 59–85, 1983.
- [30] H. T. Coelho, T. K. Das, and M. R. Robilotta, *Phys. Rev.* **C28** 1812–1828, 1983.
- [31] B. S. Pudliner, V. R. Pandharipande, J. Carlson, S. C. Pieper, and R. B. Wiringa, *Phys. Rev.* **C56** 1720–1750, 1997.
- [32] S. Weinberg, *Nucl. Phys.* **B363** 3–18, 1991.
- [33] U. van Kolck, *Phys. Rev.* **C49** 2932–2941, 1994.
- [34] J. L. Friar, D. Huber, and U. van Kolck, *Phys. Rev.* **C59** 53–58, 1999.
- [35] E. Epelbaum, A. Nogga, W. Glöckle, H. Kamada, U.-G. Meißner, and H. Witala, *Phys. Rev.* **C66** 064001, 2002.
- [36] V. Bernard, N. Kaiser, and U.-G. Meißner, *Int. J. Mod. Phys.* **E4** 193–346, 1995.
- [37] P. Büttiker and U.-G. Meißner, *Nucl. Phys.* **A668** 97–112, 2000.
- [38] M. Lüscher, *Commun. Math. Phys.* **104** 177, 1986.

- [39] M. Lüscher, *Commun. Math. Phys.* **105** 153–188, 1986.
- [40] M. Lüscher, *Nucl. Phys.* **B354** 531–578, 1991.
- [41] E. Epelbaum, H. Krebs, D. Lee, and U.-G. Meißner, *Eur. Phys. J.* **A41** 125–139, 2009.
- [42] W. T. H. van Oers and J. D. Seagrave, *Phys. Lett.* **B24** 562–565, 1967.
- [43] D. Gazit, S. Quaglioni, and P. Navratil, *Phys. Rev. Lett.* **103** 102502, 2009.